



# Flexible optimized coil designing method using space curves

Caoxiang Zhu(祝曹祥)<sup>1</sup>, Stuart Hudson<sup>2</sup>, Yuntao Song(宋云涛)<sup>3</sup>, Yuanxi Wan(万元熙)<sup>1</sup>

<sup>1</sup> University of Science and Technology of China, No. 96 JinZhai Road, Hefei, Anhui 230026, P. R. China

<sup>2</sup> Princeton Plasma Physics Laboratory, Princeton University, P.O. Box 451, New Jersey 08543, USA

<sup>3</sup> Institute of Plasma Physics, Chinese Academy of Sciences, Hefei, Anhui 230031, P. R. China

# Contents

I. Introduction and motivations

II. Theoretical backgrounds

III. Numerical implementation

IV. Illustrations and applications

- W7-X
- LHD
- Knotatron
- HSX

V. Conclusions

# Introduction and motivations

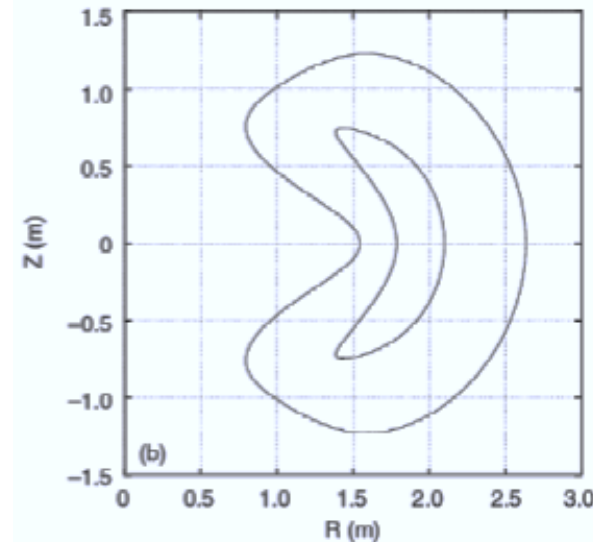
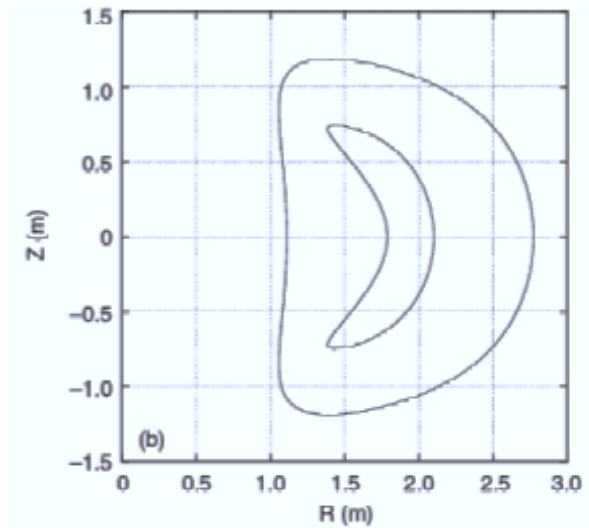
- The difficulties in designing stellarator coils have been a critical problem for long time, even partly causing the termination of NCSX [1] and the delay of the W7-X construction [2].
- The external coils that produce the required magnetic fields to support the plasma equilibrium have to meet the boundary condition of  $(\vec{B}_V + \vec{B}_p) \cdot \vec{n} = 0$  on a given plasma surface (the plasma boundary). In the vacuum region, the magnetic scalar potential satisfies the Laplace's equation  $\nabla^2 \phi = 0$ .
- The determination of coils for desired plasma boundary leads to a Cauchy-type initial value problem, which is **ill-posed** and might be impossible to be solved rigorously [3].
- But approximated solutions do existed.

# Introduction and motivations

- Pioneering work for coil design has been done by Merkel with the code NESCOIL[4], , in which he assumed that the external magnetic field is produced by a **surface current** distribution on a closed toroidal surface surrounding the plasma (“winding surface”).
- This surface current is then expressed by a current potential  $\vec{j} = \vec{n} \times \nabla \Phi$  and solved with a Green’s function method to minimize  $\epsilon^2 = \oint_{\partial S} (\vec{B} \cdot \vec{n})^2 ds$ . Then discretized coils are approximated by the contours of  $\Phi$ .
- Later, improved methods, like NESVD[5] & REGCOIL[6], and nonlinear optimizations that explicitly incorporates engineering constraints, like ONSET[7], COILOPT[8] & COILOPT++[9], have been developed.
- All the methods need a pre-defined **winding surface**.

# Introduction and motivations

- The existence of the winding surface simplifies the coil design problem. But it also introduces strong limitations.
  - “Good” winding surfaces should be provided before optimizations;
  - It’s the final coils performance that determines if a winding surface is appropriate;
  - ➔ **Nested** optimizations on both the winding surface and coils;
- A new method without the dependence of winding surface is presented here.



Optimizations of NCSX winding surface [8].

## FOCUS

Flexible Optimized Coil Using Space curves

# Theoretical backgrounds

## 1. 3D coil representation

- Single filamentary coils are closed, one-dimensional curves embedded in three-dimensional space.

$$\vec{x}(t) = x(t) \mathbf{i} + y(t) \mathbf{j} + z(t) \mathbf{k}$$

- Any representations are feasible. Here, we use a Fourier representation:

$$x(t) = X_{c,0} + \sum_{n=1}^{N_F} [X_{c,n} \cos(nt) + X_{s,n} \sin(nt)] .$$

## 2. The target function

- Coil parameters are to be varied to minimize a target function consisting of both “physics” and “engineering” objective functions,

$$\chi^2(\mathbf{X}) = \sum_j w_j \left( \frac{f_j(\mathbf{X}) - f_{j,o}}{f_{j,o}} \right)^2 ,$$

where  $\mathbf{X}$  is a set of all the variables,  $f_j(\mathbf{X})$  is the  $j^{th}$  objective function with a expected value of  $f_{j,o}$  and prescribed weight  $w_j$ .

# Theoretical backgrounds

## 3. Objective functions

- The primary objective function is to minimize the normal magnetic field errors on the desired plasma boundary,

$$f_B(\mathbf{X}) \equiv \int_S \frac{1}{2} \left( \frac{\mathbf{B} \cdot \mathbf{n}}{|\mathbf{B}|} \right)^2 ds .$$

The magnetic field at position  $\bar{\mathbf{x}}$  produced by a coils set with  $N_C$  coils is calculated using the Biot-Savart law,

$$\mathbf{B}_V(\bar{\mathbf{x}}) = \frac{\mu_0}{4\pi} \sum_{i=1}^{N_C} I_i \int_{C_i} \frac{d\mathbf{l}_i \times \mathbf{r}}{r^3} .$$

If a small deformation  $\delta \mathbf{x}_i$  is applied to the  $i^{th}$  coil, the variation on the  $f_B$  is

$$\delta f_B(\mathbf{X}) = \frac{\mu_0}{4\pi} \int_S (\mathbf{B} \cdot \mathbf{n}) I_i \int_0^{2\pi} \left[ \frac{3\mathbf{r} \cdot \mathbf{x}'_i}{r^5} \mathbf{n} \times \mathbf{r} + \frac{2}{r^3} \mathbf{x}'_i \times \mathbf{n} + \frac{3\mathbf{x}'_i \times \mathbf{r} \cdot \mathbf{n}}{r^5} \mathbf{r} \right] \cdot \delta \mathbf{x}_i dt ds^* .$$

- Objective functions with respect to the toroidal flux, length constraint, etc., can be constructed similarly,

$$f_\Psi(\mathbf{X}) \equiv \frac{1}{2\pi} \int_0^{2\pi} \frac{1}{2} \left( \frac{\Psi_\zeta - \Psi_o}{\Psi_o} \right)^2 d\zeta, \quad f_L(\mathbf{X}) = \frac{1}{N_C} \sum_{i=1}^{N_C} \frac{e^{L_i}}{e^{L_{i,o}}} .$$

\* For notational clarity, we omit the normalization term and also restrict attention to vacuum fields ( $B_p = 0$ ).

# Theoretical backgrounds

## 4. Spectral condensation and steepest descent minimization

- The parameter  $t$  in Fourier representations is not unique  $\rightarrow$  null space.
- To avoid this, additional objective function is include to minimize the spectral width  $M = \sum_i^{N_c} M_i$ , with  $M_i(\mathbf{X}) = \sum_{n=1}^{N_F} n^p (X_{c,n}^i)^2 + (X_{s,n}^i)^2 + (Y_{c,n}^i)^2 + (Y_{s,n}^i)^2 + (Z_{c,n}^i)^2 + (Z_{s,n}^i)^2$ .
- For minimizing the target function  $\chi^2$ , we apply a modified steepest descent algorithm,

$$\frac{\partial \mathbf{X}}{\partial \tau} \equiv -\frac{\partial \chi^2}{\partial \mathbf{X}} - \mathbf{X}' \left( \frac{\partial M}{\partial \mathbf{X}} \cdot \mathbf{X}' \right).$$

- The target functions is still decreasing in the usual descent direction,

$$\frac{\partial \chi^2}{\partial \tau} = \frac{\partial \chi^2}{\partial \mathbf{X}} \cdot \frac{\partial \mathbf{X}}{\partial \tau} = -\frac{\partial \chi^2}{\partial \mathbf{X}} \cdot \frac{\partial \chi^2}{\partial \mathbf{X}} - \left( \frac{\partial \chi^2}{\partial \mathbf{X}} \cdot \mathbf{X}' \right) \left( \frac{\partial M}{\partial \mathbf{X}} \cdot \mathbf{X}' \right) = -\left( \frac{\partial \chi^2}{\partial \mathbf{X}} \right)^2.$$

- Afterwards, the spectral width will be minimized in the tangential direction,

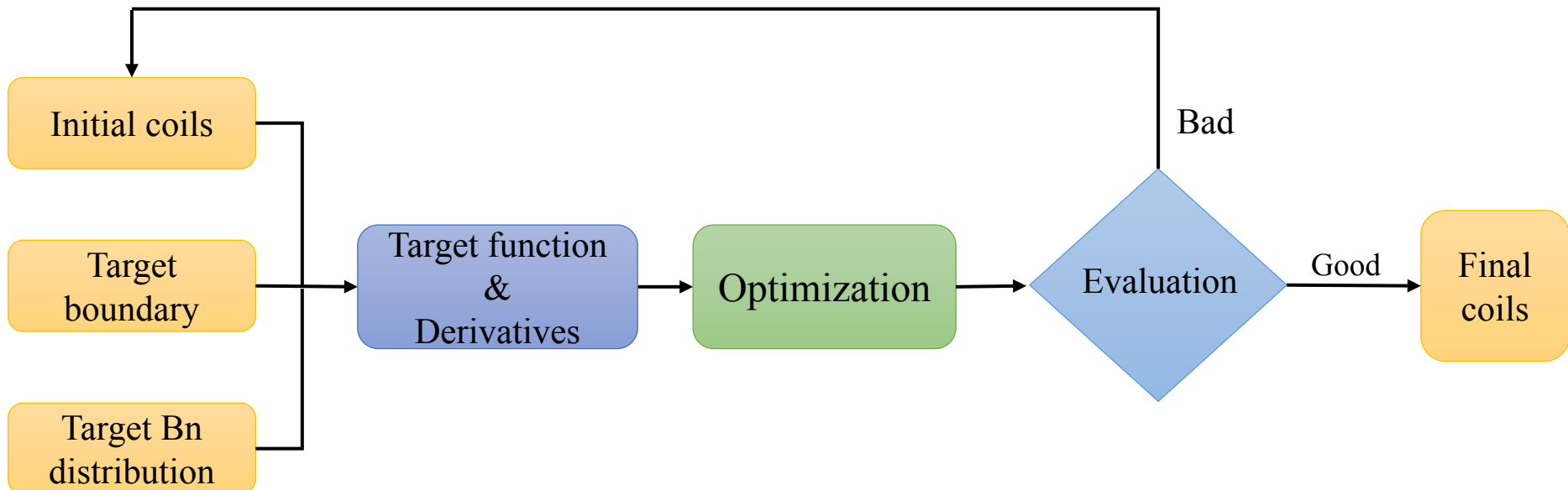
$$\frac{\partial M}{\partial \tau} = \frac{\partial M}{\partial \mathbf{X}} \cdot \frac{\partial \mathbf{X}}{\partial \tau} = -\left( \frac{\partial M}{\partial \mathbf{X}} \cdot \mathbf{X}' \right)^2.$$

# Numerical implementation

- FOCUS is written in Fortran 90, MPI enabled.
- Derivatives are calculated analytically.

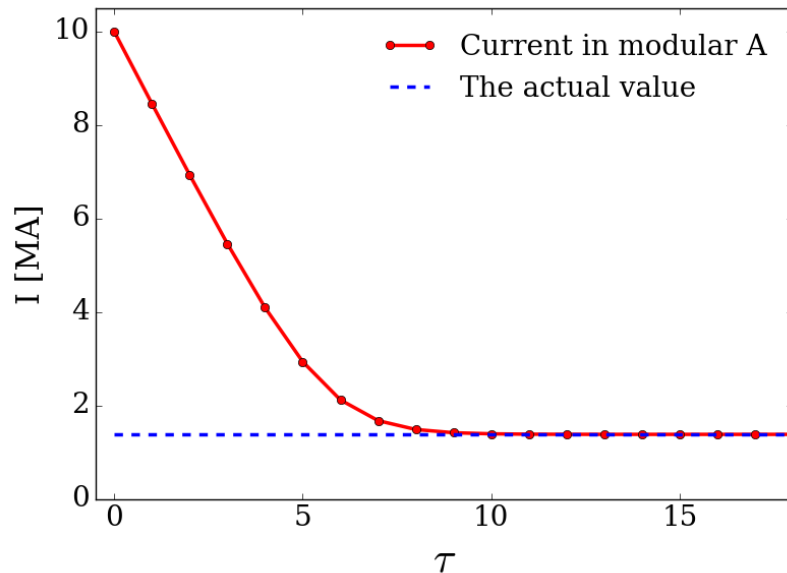
$$\frac{\partial f_B}{\partial X_{c,n}^i} \approx \sum_{j=1}^{N_\theta} \sum_{k=1}^{N_\zeta} \left[ (B_x n_x + B_y n_y + B_z n_z) \left( \frac{\partial B_x}{\partial X_{c,n}^i} n_x + \frac{\partial B_y}{\partial X_{c,n}^i} n_y + \frac{\partial B_z}{\partial X_{c,n}^i} n_z \right) \sqrt{g} \right]_{j+\frac{1}{2}, k+\frac{1}{2}} \frac{2\pi}{N_\theta} \frac{2\pi}{N_\zeta}$$

- Working flow

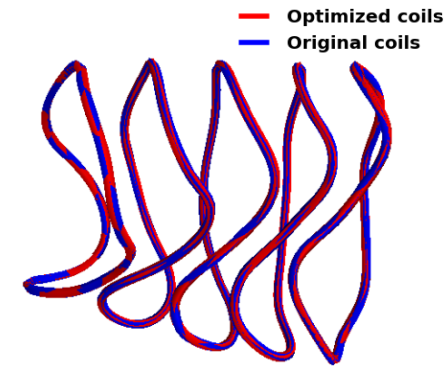


# Applications

- LCMS in the OP 1.1 limiter configuration [10] is used as the target plasma boundary.
- Primary demonstrations:
  - a) perturbing the current in one arbitrary coil and see if FOCUS can recover it;
  - b) taking the single filamentary model of real W7-X coils, fitting with Fourier representations and then optimizing the coils;



(a). FOCUS rapidly found the correct value of the perturbed current.



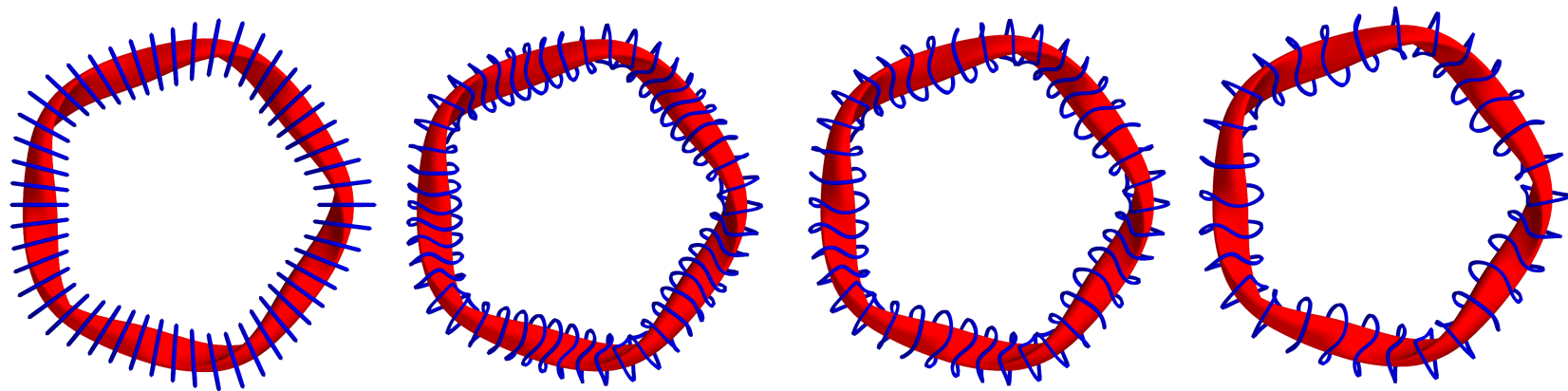
(b). The five unique shaped W7-X coils in a half period.  $f_B$  decreased from  $1.12 \times 10^{-4}$  to  $7.65 \times 10^{-5}$ ; the differences are indistinguishable at this scale.

# Applications

W7-X

- Free optimizations

Arbitrary initial guesses: circular coils that are positioned surrounding the plasma surface with equal toroidally-interval angles, varying the number of coils  $N_C$ .



Initial circular coils

$N_C = 50$

$N_C = 40$

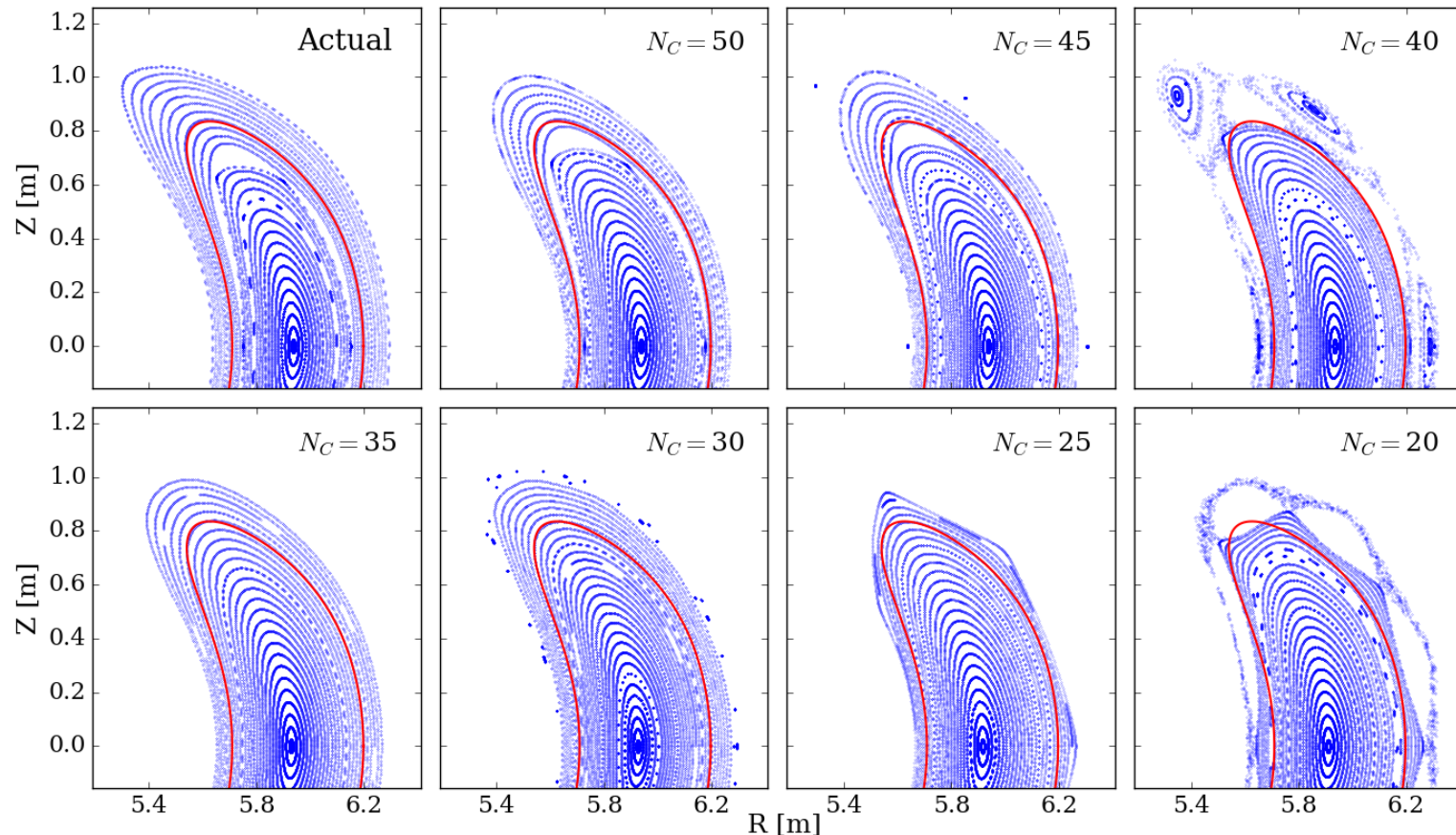
$N_C = 30$

Term	Actual coils	FOCUS coils					
		70	50	45	40	35	30
Number of coils		$1.12 \times 10^{-4}$	$1.68 \times 10^{-2}$	$1.98 \times 10^{-2}$	$3.27 \times 10^{-2}$	$5.22 \times 10^{-2}$	$8.48 \times 10^{-2}$
Squared normal field error $f_B$		$4.31 \times 10^{-7}$	$1.36 \times 10^{-2}$	$1.78 \times 10^{-3}$	$3.76 \times 10^{-3}$	$6.95 \times 10^{-3}$	$1.55 \times 10^{-2}$
Toroidal flux error $f_\Psi$							
Average length (m)	8.97	<b>6.69</b>	6.92	7.20	7.49	7.80	
Maximum curvature ( $m^{-1}$ )	<b>2.53</b>	3.22	3.05	3.03	2.84	2.55	
Minimum coil-plasma separation (m)	0.39	0.33	0.35	0.36	0.38	<b>0.41</b>	
Minimum coil-coil separation (m)	0.27	0.36	0.36	0.37	0.41	<b>0.46</b>	

Coil performance comparisons

# Applications

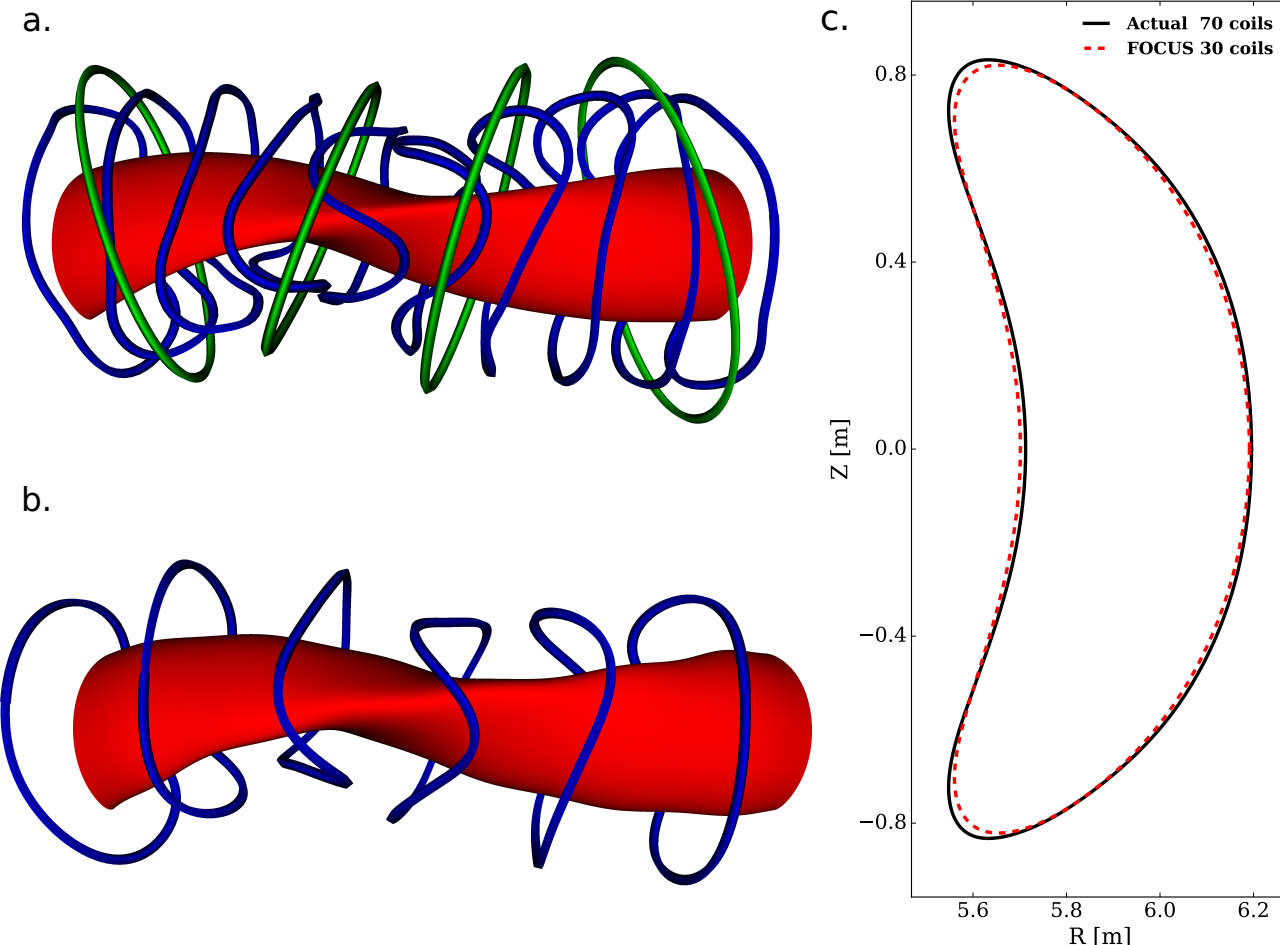
W7-X



**Poincare plots comparisons.** With enough coils ( $N_C \geq 30$ ) FOCUS can produce reasonably close agreement. The main visible difference is the  $n/m = 5/6$  island chain. For the actual coils, the  $5/6$  islands are larger and inside the target plasma boundary, whereas for FOCUS coils, these islands are slightly further out and, particularly for the cases of  $N_C=35, 30$  and  $25$ , there are no visible internal islands.

# Applications

W7-X

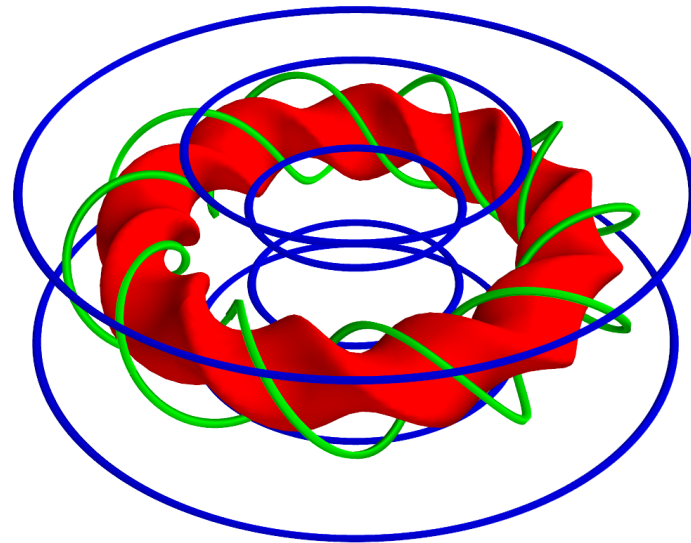


**Details about the  $N_C = 30$  case.** The free-boundary, MHD equilibrium is computed using the VMEC[12] code with zero pressure and zero plasma currents (c). The results indicate that the two coils sets have comparatively close plasma boundaries. Although small differences at the plasma boundary might have significant impacts to plasma properties, this is remained for future work.

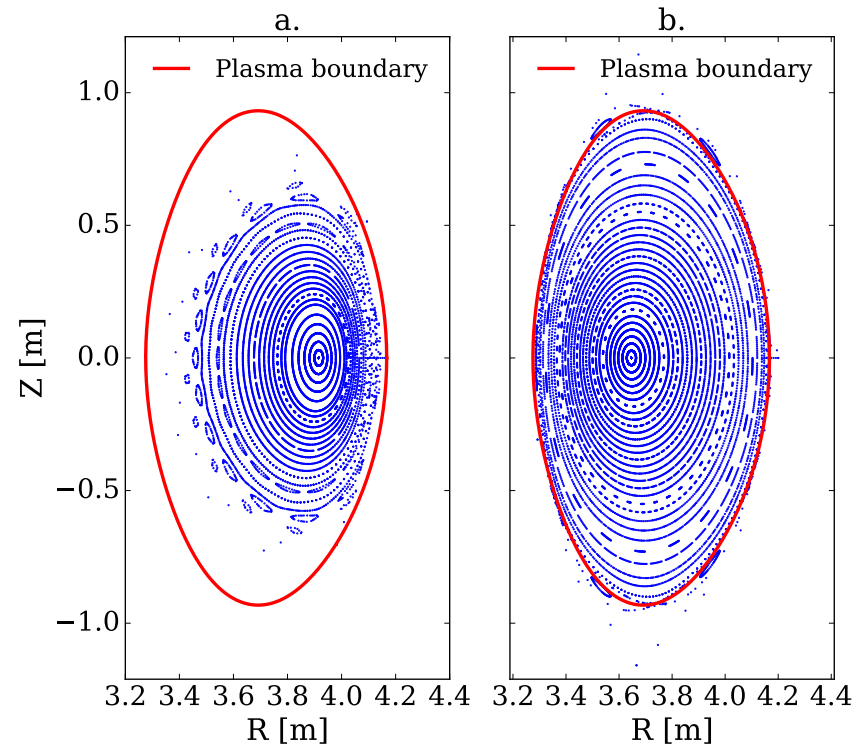
# Applications

LHD

- The LHD [11] can be approximated by two helical windings, together with three pairs of vertical field coils.
- None of the existing codes have been used to optimize helical coils.
- FOCUS can easily represent the helical and vertical field coils with Fourier representations.



The LHD coils (simplified as filaments) including two helical windings (green) and six vertical coils (blue).

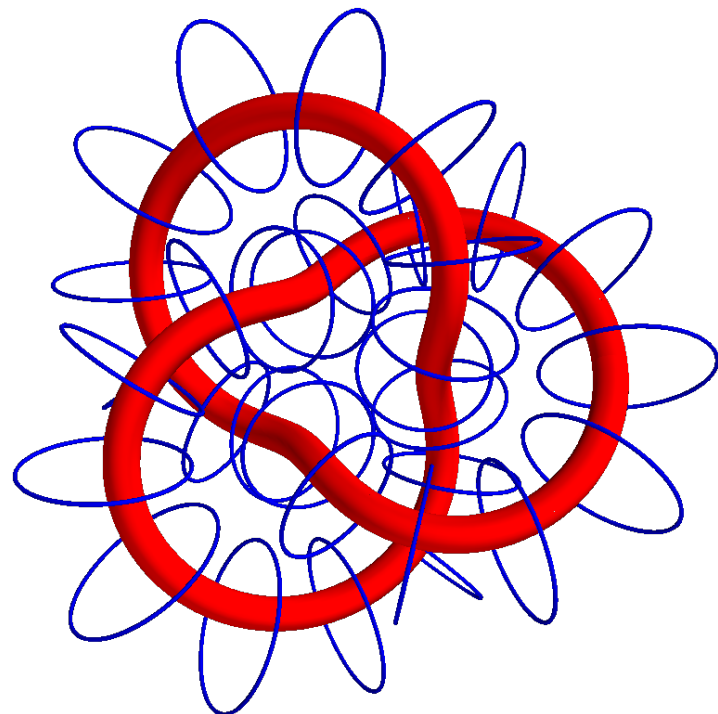


**FOCUS optimizes the helical coils.** When using Fourier representation to fit the LHD filaments, errors introduced and this results in big changes of the produced flux surfaces (a). FOCUS optimization successfully fixed the errors and got good approximation to the plasma boundary (b).

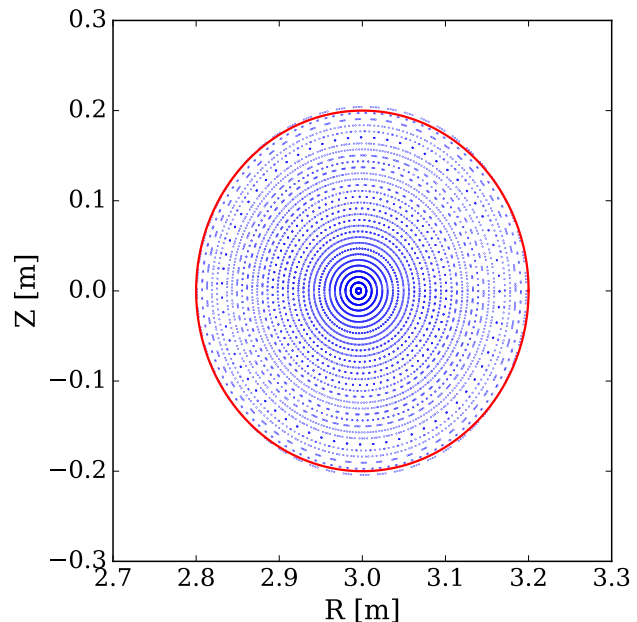
# Applications

## Knotatron

**Knotatron** [12] is a conceptual plasma configuration, with a magnetic axis in the shape of a knot. FOCUS is applied to design coils for a (2,3) knotatron, to demonstrate the code's flexibilities.



The plasma and designed coils for a  $(p,q)=(2,3)$  knotatron.

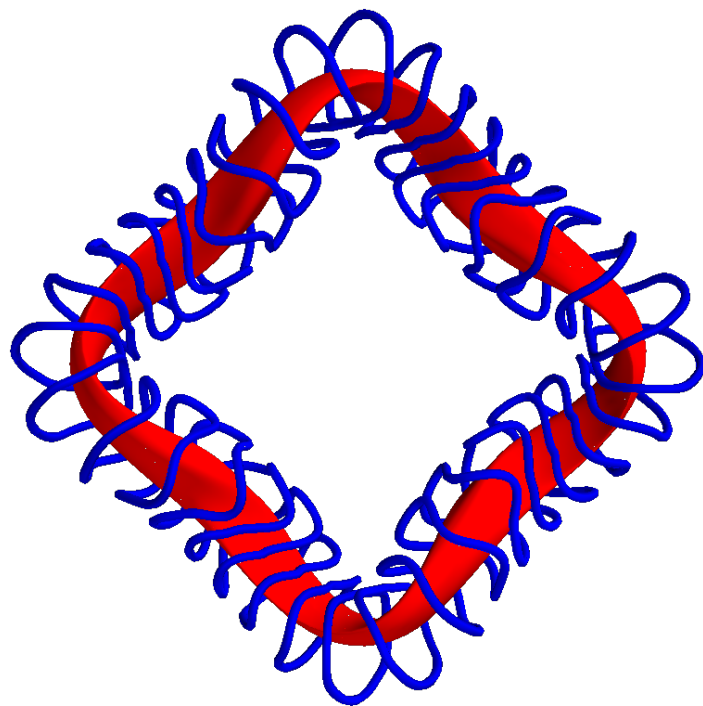


Poincare plots at one of the intersections with the x-z plane.

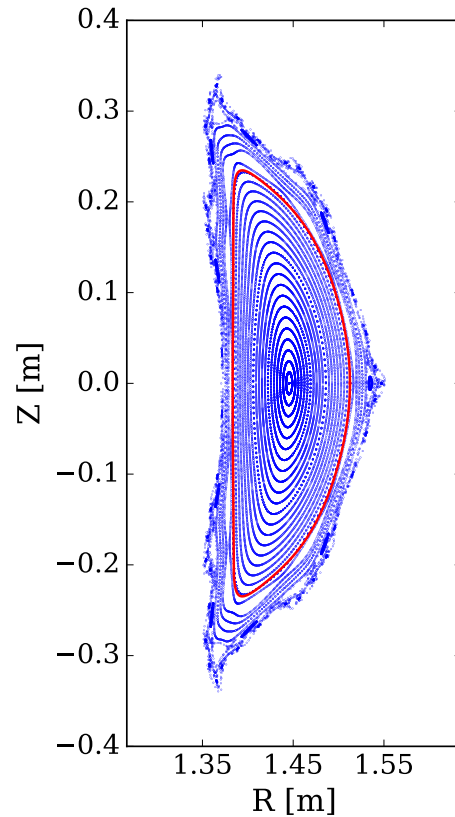
# Applications

HSX

**HSX** [13] is a quasi-helically symmetric (QHS) stellarator at the University of Wisconsin-Madison. The device has a unique magnetic field with only helical dominant component. It has 48 modular coils. Here, we are using FOCUS to design coils for HSX starting with 36 circular coils.



The 36 FOCUS optimized coils for HSX.



Poincare plots for the vacuum field at  $\zeta = 0$  plane.

# Conclusions

## Conclusions:

- The winding surface is not essential to coil designs;
- FOCUS can be used for different configurations and it's really flexible and robust;
- By getting rid of the winding surface, the FOCUS code has the potential to find out more feasible coil solutions.

## Future work to be explored:

- ❑ Directly optimizing resonant perturbation terms;
- ❑ Newton-like minimization methods;
- ❑ Capability for RMP coils in tokamaks.

# References

1. Neilson, G. H., Gruber, C. O., Harris, J. H., Rej, D. J., Simmons, R. T., & Strykowsky, R. L. (2010). Lessons learned in risk management on NCSX. *IEEE Transactions on Plasma Science*, 38(3), 320-327.
2. Riße, K. (2009). Experiences from design and production of Wendelstein 7-X magnets. *Fusion Engineering and Design*, 84(7), 1619-1622.
3. Boozer, A. H. (2005). Physics of magnetically confined plasmas. *Reviews of modern physics*, 76(4), 1071.
4. Merkel, P. (1987). Solution of stellarator boundary value problems with external currents. *Nuclear Fusion*, 27(5), 867.
5. Pomphrey, N., Berry, L., Boozer, A., Brooks, A., Hatcher, R. E., Hirshman, S. P., ... & Strickler, D. J. (2001). Innovations in compact stellarator coil design. *Nuclear fusion*, 41(3), 339.
6. Landreman, M. (2017). An improved current potential method for fast computation of stellarator coil shapes. *Nuclear Fusion*, 57(4), 046003.
7. Drevlak, M. (1998). Automated optimization of stellarator coils. *Fusion Science and Technology*, 33(2), 106-117.
8. Strickler, D. J., Berry, L. A., & Hirshman, S. P. (2002). Designing coils for compact stellarators. *Fusion Science and Technology*, 41(2), 107-115.
9. Brown, T., Breslau, J., Gates, D., Pomphrey, N., & Zolfaghari, A. (2015, May). Engineering optimization of stellarator coils lead to improvements in device maintenance. In *Fusion Engineering (SOFE), 2015 IEEE 26th Symposium on* (pp. 1-6). IEEE.
10. Pedersen, T. S., Andreeva, T., Bosch, H. S., Bozhenkov, S., Effenberg, F., Endler, M., ... & Hölbe, H. (2015). Plans for the first plasma operation of Wendelstein 7-X. *Nuclear Fusion*, 55(12), 126001.
11. Iiyoshi, A., Fujiwara, M., Motojima, O., Ohyabu, N., & Yamazaki, K. (1990). Design study for the large helical device. *Fusion Science and Technology*, 17(1), 169-187.
12. Hudson, S. R., Startsev, E., & Feibusch, E. (2014). A new class of magnetic confinement device in the shape of a knot. *Physics of Plasmas*, 21(1), 010705.
13. Anderson, F. S. B., Almagri, A. F., Anderson, D. T., Matthews, P. G., Talmadge, J. N., & Shohet, J. L. (1995). Helically symmetric experiment,(HSX) goals, design and status. *Fusion Technology*, 27(CONF-941182--).